

Energy-based Self-attentive Learning of Abstractive Communities for Spoken Language Understanding

Guokan Shang^{1,2}, Antoine J.-P. Tixier¹,
Michalis Vazirgiannis^{1,3}, Jean-Pierre Lorré²

¹École Polytechnique, ²Linagora, ³AUEB

Abstract

Abstractive Community Detection is an important Spoken Language Understanding task, whose goal is to group utterances in a conversation according to whether they can be jointly summarized by a common abstractive sentence. This paper provides a novel approach to this task. We first introduce a neural contextual utterance encoder featuring three types of self-attention mechanisms. We then evaluate it against multiple baselines within the powerful siamese and triplet energy-based meta-architectures. Moreover, we propose a general sampling scheme that enables the triplet architecture to capture subtle clustering patterns, such as overlapping and nested communities. Experiments on the AMI corpus show that our system improves on the state-of-the-art and that our triplet sampling scheme is effective. Code and data are publicly available¹.

1 Introduction

Today, large amounts of digital text are generated by spoken or written conversations, let them be human-human (customer service, multi-party meetings) or human-machine (chatbots, virtual assistants). Such text comes in the form of transcriptions. A transcription is a list of time-ordered text fragments called *utterances*. Unlike sentences in traditional documents, utterances are frequently associated with meta-information (e.g., speaker ID/role, dialogue act), and are often ill-formed, incomplete, and ungrammatical, due to the nature of spontaneous communication.

Abstractive summarization of conversations is an open problem in NLP. It requires the machine to gain a high-level understanding of the dialogue, in order to extract useful information and turn it into meaningful abstractive sentences. Previous work (Mehdad et al., 2013; Oya et al., 2014; Banerjee

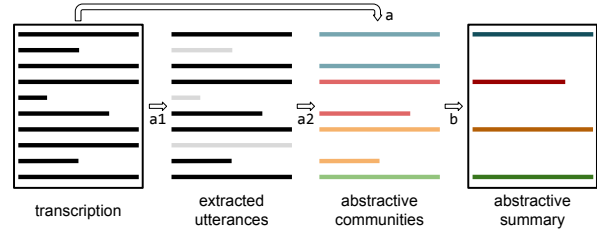


Figure 1: Abstractive Community Detection (subtask *a*) is the first step towards summarizing a conversation.

et al., 2015; Shang et al., 2018) decomposes this task into two subtasks *a* and *b* as shown in Fig. 1.

Subtask *a*, or *Abstractive Community Detection* (ACD), is the focus of this paper. It consists in grouping utterances according to whether they can be jointly summarized by a common abstractive sentence (Murray et al., 2012). Such groups of utterances are called *abstractive communities*. Once they are obtained, an abstractive sentence is generated for each group (subtask *b*), thus forming the final summary. ACD includes, but is a more general problem than, topic clustering. Indeed, as shown in Fig. 2, communities should capture more complex relationship than simple semantic similarity. Also, two utterances may be part of the same community even if they are not close to each other in the transcription. Finally, a given utterance may belong to more than one community, which results in disjoint, nested and overlapping groupings.

In this paper, we depart from previous work and argue that ACD should be broken down into two steps (*a1* and *a2* in Fig. 1). That is, summary-worthy utterances should first be extracted from the transcription (*a1*), and then, grouped into abstractive communities (*a2*). This $a1 \rightarrow a2 \rightarrow b$ process is more consistent with the way humans treat the summarization task. E.g., to create the summary of a given meeting from the sequence of utterances (successive grey nodes on the left of

¹https://bitbucket.org/guokan_shang/abscomm

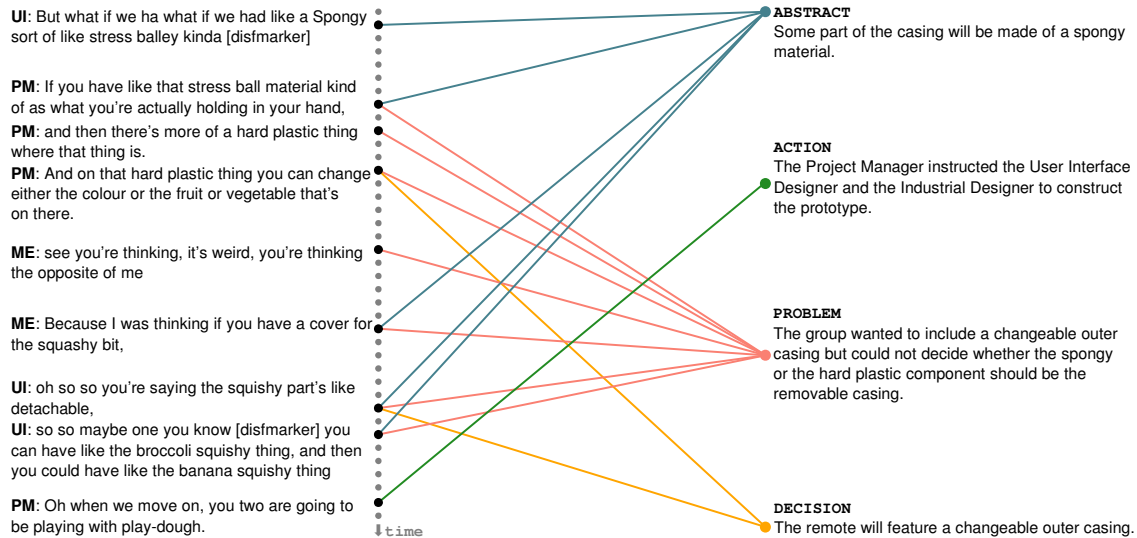


Figure 2: Example of ground truth manual annotations from the ES2011c meeting of the AMI corpus (v1.6.2). Speaker roles are PM: project manager, ME: marketing expert, and UI: user interface designer. Abstractive sentences belong to four groups: abstract, action, problem, and decision.

Fig. 2), annotators of the AMI corpus (McCowan et al., 2005) were asked to (1) write an *abstractive summary* of the meeting (right of Fig. 2), (2) extract important utterances from the transcription (black nodes on the left of Fig. 2), and (3) link utterances in the extractive summary to sentences in the abstractive summary (arrows in Fig. 2).

Step a1 plays an important filtering role, since in practice, only a small part of the original utterances are used to construct the abstractive communities (e.g., 17% on average for AMI). However, even if it is more modest as it only involves filtering, the goal of this step is closely related to *extractive summarization*, which has been extensively studied (Murray et al., 2005; Garg et al., 2009; Tixier et al., 2017).

Rather, we focus in this paper on the rarely explored a2 *utterance clustering* step, which we think is an important spoken language understanding problem, as it plays a crucial role of bridge between two major types of summaries: extractive and abstractive.

2 Departure from previous work

Prior work performed ACD either in a supervised (Murray et al., 2012; Mehdad et al., 2013) or unsupervised way (Oya et al., 2014; Banerjee et al., 2015; Singla et al., 2017; Shang et al., 2018).

In the supervised case, Murray et al. (2012) train a logistic regression classifier with hand-crafted features to predict extractive-abstractive links, then build an utterance graph whose edges

represent the binary predictions of the classifier, and finally apply an overlapping community detection algorithm to the graph. Mehdad et al. (2013) add to the previous approach by building an entailment graph for each community, where edges are entailment relations between utterances, predicted by a SVM classifier trained with hand-crafted features on an external dataset. The entailment graph allows less informative utterances to be eliminated from each community.

On the other hand, unsupervised approaches to ACD do not make use of extractive-abstractive links. Oya et al. (2014); Banerjee et al. (2015); Singla et al. (2017) assume that disjoint topic segments (Galley et al., 2003; Eisenstein and Barzilay, 2008) align with abstractive communities. Shang et al. (2018) use the classical vector space representation with TF-IDF weights. Then, they compress the utterance-term matrix with Latent Semantic Analysis, and apply k -means.

To sum up, prior ACD methods are either too complex or too simple. The former involve multiple models trained on different labeled datasets and heavily relying on handcrafted features. The latter are incapable of capturing the complicated structure of abstractive communities described in the introduction.

Motivated by the recent success of energy-based approaches to similarity learning tasks such as face verification (Schroff et al., 2015) and sentence matching (Mueller and Thyagarajan, 2016), we introduce in this paper a novel utterance en-

coder, and train it within the seminal siamese (Chopra et al., 2005) and triplet (Hoffer and Ailon, 2015) energy-based meta-architectures. Our final network is able to accurately capture the complexity of abstractive community structure, while at the same time, it is trainable in an end-to-end fashion without the need for human intervention and handcrafted features. More specifically, our contributions are fourfold:

- we apply for the first time (to the best of our knowledge) energy-based learning to a spoken language understanding task,
- we introduce a novel utterance encoder featuring three types of self-attention mechanisms and taking contextual and temporal information into account,
- we propose a sampling scheme that enables the triplet architecture to capture subtle levels of similarity between objects, such as overlapping and nested clusters. This is a major improvement over prior work, in which only the usual similar/dissimilar case is tackled.
- Through extensive experiments and ablations, we study the impact of each component and architectural choice on performance.

3 Energy-based learning

Energy-Based Modeling (EBM) (LeCun and Huang, 2005; LeCun et al., 2006) is a unified framework that can be applied to many machine learning problems. In EBM, an energy function assigns a scalar called *energy* to each pair of random variables (X, Y) . The energy can be interpreted as the incompatibility between the values of X and Y . Training consists in finding the parameters W^* of the energy function E_W that, for all (X^i, Y^i) in the training set \mathcal{S} of size P , assign low energy to compatible (correct) combinations and high energy to all other incompatible (incorrect) ones. This is done by minimizing a *loss functional*² \mathcal{L} :

$$W^* = \arg \min_{W \in \mathcal{W}} \mathcal{L}(E_W(X, Y), \mathcal{S}) \quad (1)$$

For a given X , prediction consists in finding the value of Y that minimizes the energy.

²the *loss functional* is passed the output of the energy function, unlike a *loss function* which is directly fed the output of the model.

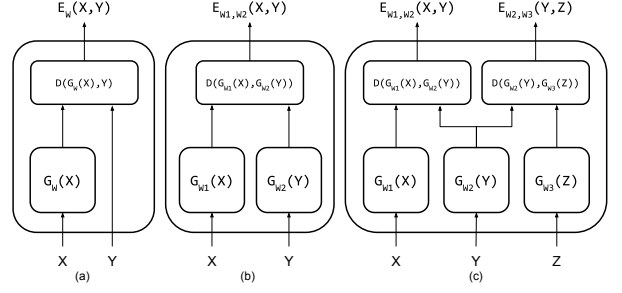


Figure 3: Three EBM architectures. When all G 's and W 's are equal, (b) and (c) correspond to the well-known siamese and triplet architectures.

3.1 Single architecture

In the EBM framework, a regression problem can be formulated as shown in Fig. 3a, where the input X is passed through a regressor model G_W and the scalar output is compared to the desired output Y with a dissimilarity measure D such as the squared error. Here, the energy function is the loss functional to be minimized.

$$\mathcal{L} = \frac{1}{P} \sum_{i=1}^P E_W(X^i, Y^i) = \frac{1}{P} \sum_{i=1}^P \|G_W(X^i) - Y^i\|^2 \quad (2)$$

Prediction is simply $Y^* = G_{W^*}(X)$.

3.2 Siamese architecture

In the regression problem previously described, the dependence between X and Y is expressed by a direct mapping $Y = f(X)$, and there is a single best Y^* for every X . However, when X and Y are not in a predictor/predictand relationship but are exchangeable instances of the same family of objects, there is no such mapping. For instance, in paraphrase identification, a sentence may be similar to many other ones, or, in language modeling, a given n -gram may be likely to be followed by many different words.

Thereby, LeCun et al. (2006) introduced EBM for *implicit regression* or *constraint satisfaction* (see Fig. 3b), in which a constraint that X and Y must satisfy is defined, and the energy function measures the extent to which that constraint is violated:

$$E_{W_1, W_2}(X, Y) = D(G_{W_1}(X), G_{W_2}(Y)) \quad (3)$$

where G_{W_2} and G_{W_1} are two functions parameterized by W_1 and W_2 . When $G_{W_1} = G_{W_2}$ and $W_1 = W_2$, we obtain the well-known siamese architecture (Bromley et al., 1994; Chopra et al.,

2005), which has been applied with success to many tasks, including sentence similarity (Mueller and Thyagarajan, 2016).

Here, the constraint is determined by a collection-level set of binary labels. For instance, $((X^i, Y^i), 0)$ indicates that (X^i, Y^i) is a *genuine* pair (e.g. two paraphrases), while $((X^i, Y^i), 1)$ indicates that (X^i, Y^i) is an *impostor* pair (e.g. two sentences with different meanings).

The function G_W projects objects into an embedding space such that the defined dissimilarity measure D (e.g., Euclidean distance) in that space reflects the notion of dissimilarity in the input space. Thus, the energy function can be seen as a metric to be learned.

In our study, we experiment with various deep neural networks encoders as the function G_W (see next section). Moreover, following (Mueller and Thyagarajan, 2016), we adopt the exponential negative manhattan distance as dissimilarity measure, and the mean squared error as loss functional:

$$E_W(X, Y) = 1 - \exp(-\|G_W(X) - G_W(Y)\|_1)$$

$$\mathcal{L} = \frac{1}{P} \sum_{i=1}^P \|E_W(X^i, Y^i) - C^i\|^2 \quad (4)$$

3.3 Triplet architecture

The triplet architecture (Schroff et al., 2015; Hoffer and Ailon, 2015; Wang et al., 2014), as can be seen in Fig. 3c, is a direct extension of the siamese architecture that takes as input a triplet (X, Y, Z) in lieu of a pair (X, Y) . X , Y , and Z are referred to as the *positive*, *anchor*, and *negative* objects, respectively. X and Y are similar, and both are dissimilar to Z . Learning consists in jointly minimizing the positive-anchor energy $E_W(X^i, Y^i)$ and maximizing the anchor-negative energy $E_W(Y^i, Z^i)$.

In this paper, we use the *softmax triplet loss* (Hoffer and Ailon, 2015) as our loss functional:

$$\mathcal{L} = \frac{1}{2P} \sum_{i=1}^P (\|ne^+ - 0\|^2 + \|ne^- - 1\|^2) \quad (5)$$

$$ne^+ = \frac{e^{E_W(X^i, Y^i)}}{e^{E_W(X^i, Y^i)} + e^{E_W(Y^i, Z^i)}} \quad (6)$$

$$ne^- = \frac{e^{E_W(Y^i, Z^i)}}{e^{E_W(X^i, Y^i)} + e^{E_W(Y^i, Z^i)}} \quad (7)$$

where ne stands for normalized energy, and the dissimilarity measure is the Euclidean distance,

i.e., $E_W(X^i, Y^i) = \|G_W(X^i) - G_W(Y^i)\|_2$. Essentially, the softmax triplet loss is the mean squared error between the normalized energy vector $[ne^+, ne^-]$ and $[0, 1]$.

3.4 On our choice of loss functionals

The softmax triplet loss (STL) performed better in our experiments than the margin-based loss used in (Schroff et al., 2015) and (Wang et al., 2014). One of the reasons may be that STL is able to capture a finer notion of distance. Indeed, with a margin-based loss, the Euclidean distance between the anchor and the negative (let us compactly denote it as d^-) need to satisfy $d^- > d^+ + m$, where m is the margin (see Fig. 4a). In other words, the distance between the positive and the negative is at least m (when all three points are aligned).

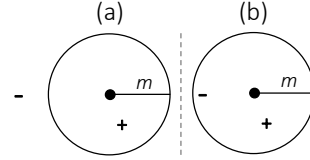


Figure 4: •, -, + denote anchor, negative, and positive.

However, the objective of STL is simply $d^- > d^+$, without imposing an absolute lower bound on the distance between positives and negatives (i.e., only the distance ratio is of interest, see Fig. 4b), which gives more freedom to the model.

To be consistent, we adopt the loss functional equipped with the dissimilarity measure (see Equation 4) for the Siamese architecture, because it also does not require a pre-defined hard margin, unlike the conventional contrastive loss functional in (Chopra et al., 2005; Neculoiu et al., 2016).

3.5 Sampling procedures

Pair sampling. All utterances belonging to the same community are paired as genuine pairs, while impostor pairs any two utterances coming from different communities.

Triplet sampling. The property of STL previously described allows us to propose a novel, flexible sampling scheme that enables fine patterns, such as overlapping and nested groupings, to be learned. Full details are provided in Appendix A).

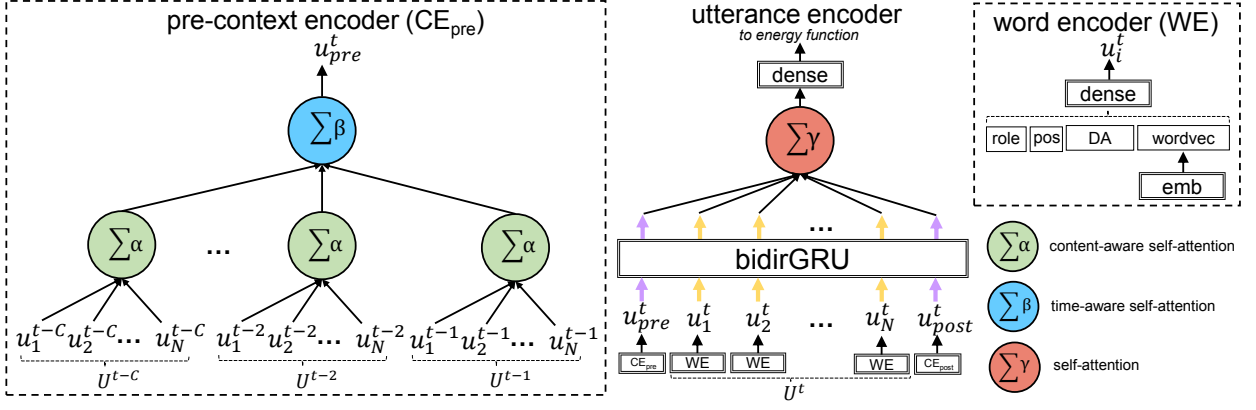


Figure 5: Our proposed utterance encoder. Only the pre-context encoder is shown. C is the context size.

4 Proposed utterance encoder

4.1 Notation

Throughout this paper, the *time* t (as superscript) denotes the position of a given utterance in the conversation of length T , and the *position* i (as subscript) denotes the position of a token within a given utterance. For instance, \mathbf{u}_1^t is the representation of the first token of \mathbf{U}^t , the t^{th} utterance in the transcription. Upper and lower case is used for matrices and vectors, respectively. Vectors are distinguished from floats by using boldface.

4.2 Word encoder

As shown in the upper right corner of Fig. 5, we obtain \mathbf{u}_i^t by concatenating the pre-trained vector of the corresponding token with the discourse features of \mathbf{U}^t (role, position and dialogue act), and passing the resulting vector to a dense layer.

4.3 Utterance encoder

As shown in the center of Fig. 5, we represent \mathbf{U}^t as a sequence of N d -dimensional token representations $\{\mathbf{u}_1^t, \dots, \mathbf{u}_N^t\}$. N is assumed (without loss of generality) to be constant at the corpus level. In addition, because there is a strong time dependence between utterances (see Fig. 2), we inform the model about the preceding and following utterances when encoding \mathbf{U}^t . To accomplish this, we use an approach inspired by the input-feeding method of (Luong et al., 2015) for Neural Machine Translation. In (Luong et al., 2015), at each time step, the previous attentional vector is concatenated with the current input to make the model aware of past alignment decisions. In our encoder-only setting, we prepend (resp. append) to \mathbf{U}^t a context vector containing information about the

previous (resp. next) utterances, finally obtaining $\mathbf{U}^t = \{\mathbf{u}_{pre}^t, \mathbf{u}_1^t, \dots, \mathbf{u}_N^t, \mathbf{u}_{post}^t\} \in \mathbb{R}^{(N+2) \times d}$.

We then use a non-stacked bidirectional Recurrent Neural Network (RNN) with Gated Recurrent Units (GRU) (Cho et al., 2014) to transform \mathbf{U}^t into a sequence of annotations $\mathbf{H}^t \in \mathbb{R}^{(N+2) \times 2d}$. In practice, the pre and post context vectors initialize the left-to-right and right-to-left RNNs with information about the utterances preceding and following \mathbf{U}^t . How we derive the pre and post context vectors is explained in subsection 4.4.

Self-attention. The self-attention mechanism (Vaswani et al., 2017; Lin et al., 2017; Yang et al., 2016), also called *inner* or *intra* attention, emerged in the literature following the success of attention in the sequence-to-sequence setting (Bahdanau et al., 2014; Luong et al., 2015). While self-attention deals with a single source sequence (no decoder), the motivation is the same as with traditional attention: rather than considering the last annotation of the RNN encoder as a summary of the entire input sequence, which is prone to information loss, a new hidden representation is computed as a weighted sum of the annotations at *all* positions, where the weights are computed by a trainable mechanism that performs a comparison operation.

While in seq2seq, the comparison involves the transformed input and the current hidden state of the decoder, in the encoder-only setting, the annotations \mathbf{H}^t are passed through a dense layer and compared (dot product) with a trainable vector \mathbf{u}_γ , initialized randomly. Then, a probability distribution over the N tokens in \mathbf{U}^t is obtained via a softmax:

$$\gamma^t = \text{softmax}(\mathbf{u}_\gamma \cdot \tanh(\mathbf{W}_\gamma \mathbf{H}^t)) \quad (8)$$

(bias omitted for readability). The attentional vec-

tor for \mathbf{U}^t is finally computed as a weighted sum of its annotations, and is passed to a dense layer to obtain the final utterance embedding $\mathbf{u}^t \in \mathbb{R}^{d_f}$:

$$\mathbf{u}^t = \text{dense} \left(\sum_{i=1}^{N+2} \gamma_i^t h_i^t \right) \quad (9)$$

\mathbf{u}_γ replaces the hidden state of the decoder in the traditional attention mechanism. It can be interpreted as a learned representation of the “ideal” word, on average. The more similar a token vector is to this representation, the more attention the model pays to the token.

4.4 Context encoder: level 1

We now explain how we derive the pre and post context vectors that we prepend and append to \mathbf{U}^t so as to inject contextual information into the encoding process. They are obtained by aggregating information from the C utterances preceding and following \mathbf{U}^t (respectively):

$$\mathbf{u}_{\text{pre}}^t \leftarrow \text{aggregate}_{\text{pre}}(\{\mathbf{U}^{t-C}, \dots, \mathbf{U}^{t-1}\}) \quad (10)$$

$$\mathbf{u}_{\text{post}}^t \leftarrow \text{aggregate}_{\text{post}}(\{\mathbf{U}^{t+1}, \dots, \mathbf{U}^{t+C}\}) \quad (11)$$

where C , the context size, is a hyperparameter. Since $\mathbf{u}_{\text{pre}}^t$ and $\mathbf{u}_{\text{post}}^t$ will become part of utterance \mathbf{U}^t which is a sequence of token vectors, and fed to the RNN, we need them to live in the same space as any other token vector. This forbids the use of any nonlinear or dimension-changing transformation in aggregate, such as convolutional or recurrent operations. Therefore, we use self-attention only. More precisely, we propose a two-level hierarchical architecture that makes use of a different type of self-attention at each level (see left part of Fig. 5). The pre and post context encoders share the exact same architecture, so we only describe the pre-context encoder in what follows.

Content-aware self-attention. At the first level, we apply the same attention mechanism to each utterance in $\{\mathbf{U}^{t-C}, \dots, \mathbf{U}^{t-1}\}$. Let us consider \mathbf{U}^{t-1} for instance. We have:

$$\boldsymbol{\alpha}^{t-1} = \text{softmax} \left(\mathbf{u}_\alpha \cdot \tanh \left(\mathbf{W}_\alpha \mathbf{U}^{t-1} + \mathbf{W}' \sum_{i=1}^N \mathbf{u}_i^{t-1} \right) \right) \quad (12)$$

This mechanism is the same as in Eq. 8, except for two differences. First, we operate directly on the matrix of token vectors \mathbf{U}^{t-1} rather than on RNN annotations. Second, there is an extra input

that consists of the element-wise sum of the word vectors of \mathbf{U}^t .

The latter modification is inspired by the coverage vector used in the seq2seq summarization model of (See et al., 2017), which is the sum of the attentional distributions over all previous steps of the decoder. Its role is to decrease repetition in the final summary, by letting the attention mechanism know which information about the source document has already been captured, in the hope that the model will focus on other aspects of it. In our case, we hope that by letting the model know about the tokens in \mathbf{U}^t , it will be able to extract complementary (rather than redundant) information from the context of \mathbf{U}^t , and thus produce a richer embedding for it.

Bi-directional information pathway. To recapitulate, we consider \mathbf{U}^t when computing $\mathbf{u}_{\text{pre}}^t$ and $\mathbf{u}_{\text{post}}^t$, and then prepend/append these vectors to \mathbf{U}^t when encoding it. Therefore, in effect, information first flows from the current utterance to its context to guide context encoding, and then flows back to the current utterance to inform its encoding.

Weight sharing. The same content-aware self-attention mechanism is applied to the entire context surrounding \mathbf{U}^t , that is, to all preceding and following utterances. We did experiment with separate pre/post mechanisms, without significant improvements. This makes sense, as there is no inherent difference between preceding and following utterances. Indeed, the latter become the former as we slide the window over the transcription from start to finish. In addition, sharing weights makes for a more parsimonious and faster model. One should note, however, that the pre and post context encoders still differ in terms of their time-aware attention mechanisms (at level 2).

Dimensionality reduction. The content-aware attention mechanism transforms the sequence of utterance matrices $\{\mathbf{U}^{t-C}, \dots, \mathbf{U}^{t-1}\} \in \mathbb{R}^{C \times N \times d}$ into a sequence of vectors $\{\mathbf{u}^{t-C}, \dots, \mathbf{u}^{t-1}\} \in \mathbb{R}^{C \times d}$. These vectors are then aggregated into a single pre-context vector $\mathbf{u}_{\text{pre}}^t \in \mathbb{R}^d$ as described next.

4.5 Context encoder: level 2

As can be inferred from Fig. 2, there is a strong time dependence between utterances in conversational speech. That is, two utterances close to each other in time are much more likely to be related

(e.g., question/answer, elaboration...) than any two randomly selected utterances. To enable our model to capture such a notion, we used the trainable universal time-decay attention mechanism of (Su et al., 2018).

Time-aware self-attention. The mechanism combines three types of time-decay functions via weights w_i . E.g., the attentional coefficient for \mathbf{u}^{t-1} is computed as follows:

$$\begin{aligned}\beta^{t-1} &= w_1\beta^{\text{conv}^{t-1}} + w_2\beta^{\text{lin}^{t-1}} + w_3\beta^{\text{conc}^{t-1}} \\ &= \frac{w_1}{a(d^{t-1})^b} + w_2[ed^{t-1} + k]^+ + \frac{w_3}{1 + \left(\frac{d^{t-1}}{D_0}\right)^l}\end{aligned}\quad (13)$$

where $[*]^+ = \max(*, 0)$ (ReLU), d^{t-1} is the offset between the positions of \mathbf{U}^{t-1} and \mathbf{U}^t , i.e., $d^{t-1} = |t - (t-1)| = 1$, and the w_i 's, a , b , e , k , D_0 , and l are scalar parameters learned during training.

Each of the three terms models a different type of time dependence. The `convex` function assumes that its decreases very quickly, `linear` assumes a linear decline, and `concave` assumes a slow decay.

Note that the time-aware self-attention mechanism can be obtained by symmetry, and has different parameters. To sum up, across the utterance and the context encoders, our architecture makes use of three different attention mechanisms.

5 Community detection

Once a transcription has been processed by our model, all utterances live in a compact space. The assumption we make is that if training was successful, the Euclidean distance in that space captures community structure, so that a simple clustering algorithm such as k -means (MacQueen, 1967) is enough to perform community detection.

Since we need to detect overlapping communities however, we use a probabilistic version of k -means, the Fuzzy c-Means (FCM) algorithm (Bezdek et al., 1984). FCM returns a probability distribution over all communities for each utterance. More details are provided in Appendix C.

6 Experiments

6.1 Dataset

The AMI corpus (McCowan et al., 2005) contains data for more than 100 meetings, in which participants play 4 roles within a design team whose

type	abstract	action	problem	decision	total
unique	1147	247	380	594	2368
disjoint	528	124	69	45	766
nested	96	106	200	437	839
overlapping	349	17	163	149	678
singleton	49	162	38	244	493

Table 1: Statistics of abstractive communities

task is to develop a prototype of TV remote control. Each meeting is associated with the annotations described in Section 1 and shown in Fig. 2. The corpus contains 2368 unique abstractive communities, whose statistics are shown in Table 1. We adopt the officially suggested *scenario-only partition*³, which provides 97, 20, and 20 meetings respectively for training, validation and testing. We do not apply any particular preprocessing except filtering out specific ASR tags, such as `vocalsound`.

6.2 Baselines

We evaluate our utterance encoder against multiple strong baselines, briefly presented next.

- **LD** (Lee and Derroncourt, 2016). A sequential sentence encoder developed for dialogue act classification. The model only leverages a limited number of utterances in preceding context when classifying the current one. Sentence representations are combined with a particular aggregation layer through two-level architectures.
- **HAN** (Yang et al., 2016). The Hierarchical Attention Network, developed for document classification, applies a self-attentive bidirectional RNN (with GRU units) to each sentence independently to get a sequence of sentence vectors. Then, the same encoder (with different parameters) is used to produce a document embedding from the sentence vectors.
- **TF-IDF**. A TF-IDF vector is used as the utterance embedding, compressed to a dimension of 21 with PCA (for reasons that will become clear in subsection 6.3), concatenated with the discourse features into a d -dimensional vector, and then compressed to a d_f -dimensional vector with PCA.
- **word2vec**. Identical to the previous baseline, but using the average of the `word2vec` vectors of the utterance tokens as its embedding.

We also considered 4 variants of our model, to measure the respective impact on performance of its various components.

³<http://groups.inf.ed.ac.uk/ami/corpus/datasets.shtml>

- **Our Model (CE-S)**: we replace the time-aware self-attention mechanism of the context encoder with basic self-attention.
- **Our Model (S-S)**: we replace both the content-aware and the time-aware self-attention mechanisms of the context encoder with basic self-attention.
- **Our Model (0,0)**: our model, without using the contextual encoder.
- **Our Model (3,0)**: our model, using only pre-context, with a small window of 3, to enable fair comparison with the LD baseline.

6.3 Experimental setup

Word encoder. Discourse features consist of two one-hot vectors of dimensions 4 and 16, respectively for speaker role and dialogue act. The positional feature is a scalar in $[0, 1]$, indicating the normalized position of the utterance in the transcription. We used the pre-trained vectors learned on the Google News corpus with `word2vec` by (Mikolov et al., 2013), and randomly initialized out-of-vocabulary words (1645 out of 12412). Note that as a preprocessing step, we reduced the dimensionality of the pre-trained word vectors from 300 to 21 with PCA, in order to give equal importance to discourse and textual features. In the end, tokens are thus represented by a $d = 42$ -dimensional vector.

Note that these token representations are used by our model and its variants, but also by the LD and HAN baselines, to be fair.

Layer sizes. For our model, and the LD and HAN baselines, we set $d_f = 32$ (output dimension of the final dense layer).

LD. We set $d_1 = 3$, $d_2 = 0$, which is very close to $(2, 0)$, the best configuration reported in the original paper.

HAN. Again, for the sake of fairness, we give the HAN baseline access to contextual information, by feeding it the current utterance surrounded by the C_b preceding and C_b following utterances in the transcription, where C_b denotes the best context size found in Subsection 7.1.

Optimization. Note that the same settings were used for our model, its variants, and the baselines. We trained for 30 epochs with the Adam (Kingma and Ba, 2014) optimizer. The best epoch was selected as the one associated with the lowest validation loss. Batch size and dropout (Srivastava et al., 2014) were set to 16 and 0.5, respectively.

Dropout was applied to the word embedding layer only. To account for the randomness of the procedure, we report average performance over 10 runs.

6.4 Tuple subsampling and resampling

When labeled tuples (pairs or triplets) are not provided, but must be constructed from the dataset, subsampling is critical for training a model within the siamese or triplet meta-architectures. For instance, in face verification (Chopra et al., 2005), a virtually infinite number of impostor pairs can be constructed, while only a limited number of genuine pairs are available. Usually, one selects $n \geq 1$ times more impostor pairs than genuine pairs, but n must not be too large to avoid large imbalance (Chopra et al., 2005; Neculoiu et al., 2016). Subsampling is also a critical issue for triplets (Wang et al., 2014; Schroff et al., 2015; Amos et al., 2016).

Following (Hoffer and Ailon, 2015; Liu et al., 2019), at the beginning of each epoch, we sample one triplet from each pair of communities belonging to the same meeting, using the strategy explained in Subsection 3.5. We thus obtain 15594 training triplets. This intelligently maximizes data usage while preventing overfitting. We used the same approach for siamese. To allow for a fair comparison, 15594 genuine pairs and 15594 impostor pairs were sampled at the beginning of each epoch, since we consider that one triplet essentially equates one genuine pair and one impostor pair.

While we used resampling for training tuples, we used a single fixed validation set across epochs, which consisted in 2891 triplets/5782 pairs. Note that we do not need to sample any pair or triplet from the test set. On the test set, we just get a vector for each utterance by feeding them to the trained model G_W .

6.5 Performance metrics

We evaluate performance at two levels.

Metric learning. First, we test whether the distance in the final embedding space is meaningful. To do so, for a given *query* utterance, we rank all other utterances in decreasing order of similarity with the query. We then use precision, recall, and F1 score at k to evaluate the quality of the ranking. A detailed example is provided in Appendix D.

The same procedure is repeated for all utterances. To account for differences in community

size, scores are first averaged at the community-level, and then at the meeting-level. Note that the distance is Euclidean for triplet and Manhattan for siamese (see subsections 3.2 and 3.3).

Singleton communities are excluded from the evaluation at this stage. We set $k = 10$, which is equal to the average number of non-singleton communities minus one (since the query utterance cannot be part of the results).

We also report results for $k = v$, that is, k is equal to the size of the community of the query utterance minus one. In that case, P, R , and $F1$ are all equal.

Clustering. Second, we compare our community assignments to the human ground truth using the Omega-Index (Collins and Dent, 1988), a standard metric for comparing non-disjoint clustering, used in the ACD literature (Murray et al., 2012). More details about the Omega-Index are provided in Appendix E.

Since FCM yields a probability distribution over communities for each utterance, we need to use a threshold to assign a given utterance to one or more communities. We selected 0.2 after trying multiple values in $[0, 0.5]$ with steps of 0.05 on the validation set. Whenever one or more utterances are not assigned to any community, we merge them into a new community.

Also, since FCM does not return nested groupings, we merged the ground truth communities nested under the same community, in order to allow for a fair comparison.

Furthermore, we set the number of clusters $|Q|$ to 11, which corresponds to the average number of ground truth communities per meeting (after merging). We also report results supposing that the number of communities is known for each test meeting (denoted in what follows as the $|Q| = v$ case).

7 Results

7.1 Context size

The context size C is a hyperparameter. Intuitively, larger contexts bring richer information, allowing a better understanding of the current utterance, but they also increase the risk of considering completely unrelated utterances. Whether the pre-context or the post-context is most important was also to be discovered.

Therefore, we tried different values of C on the validation set, under two settings: (pre, post) = $(C, 0)$, and (pre, post) = (C, C) .

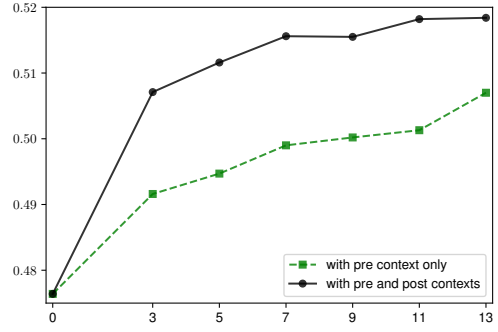


Figure 6: Impact of context size on performance for $P@k = v$ on the validation set. Results look similar for $F1@k = 10$.

Results are shown in Fig. 6. We can observe that increasing C always brings improvement, with diminishing returns. Results also clearly show that considering the following utterances is useful. Therefore, we select (11, 11) as our best context sizes.

7.2 Comparison with baselines

Results are shown in Table 2 for the triplet (rows a-b-c) and siamese (rows h-i-j) frameworks.

Our Model (3,0) significantly outperforms *LD* (rows f and m) under both the siamese and triplet configuration. Also, *Our Model* and its variants using best context sizes perform better than HAN (rows g and n) everywhere, except for the $P@k = v$ metric in the siamese configuration.

TF-IDF and *word2vec* (rows o and p) perform significantly worse than all EBM models, *word2vec* is better than TF-IDF, which is expected.

Also, all variants of our model using best context size (11,11) outperform the ones using reduced (3,0) or no (0,0) context, regardless of the configuration. This confirms the value added by our context encoder.

For the Triplet architecture (rows c, d, e), *Our Model* (CE-S) achieves best performance on all scores except the Omega Index when $|Q| = 11$. For the Siamese architecture (rows j, k, l), *Our Model* outperforms two variants in terms of all metrics employed. Overall, these results demonstrate that the models adopt content-aware self-attention mechanism at the place of α are consistently better throughout the different architectures.

7.3 Attention visualization

To understand how the three self-attention mechanisms work together, we visualize their behaviors with an example (see Appendix B). The example

			(pre, post)	P	P	R	F1	Omega Index			
				@ <i>k</i> = <i>v</i>	@ <i>k</i> = 10			<i>Q</i> = <i>v</i>	<i>Q</i> = 11		
Triplet architecture	a)	Our Model	(0, 0)	54.59	46.05	62.45	43.18	49.09	48.81		
	b)	Our Model	(3, 0)	55.17	46.17	62.80	43.25	49.78	49.70		
	c)	Our Model	(11, 11)	58.58	46.73	63.82	43.83	49.90	49.28		
	d)	Our Model (CE-S)	(11, 11)	59.52*	46.98*	64.01*	44.06*	50.11	49.73		
	e)	Our Model (S-S)	(11, 11)	58.96	46.81	63.65	43.87	49.59	49.88		
	f)	LD	(3, 0)	52.04	44.82	60.41	41.82	48.70	48.14		
	g)	HAN	(11, 11)	58.72	45.76	62.60	42.89	49.32	48.88		
Siamese architecture	h)	Our Model	(0, 0)	53.01	45.10	60.97	42.12	50.56	49.65		
	i)	Our Model	(3, 0)	53.78	45.54	61.33	42.48	51.01	50.00		
	j)	Our Model	(11, 11)	56.64	46.47	62.54	43.40	52.44*	51.88*		
	k)	Our Model (CE-S)	(11, 11)	56.46	46.08	61.92	43.02	51.60	50.98		
	l)	Our Model (S-S)	(11, 11)	55.68	45.64	61.17	42.53	52.26	51.11		
	m)	LD	(3, 0)	52.13	44.83	60.85	41.86	51.18	50.70		
	n)	HAN	(11, 11)	58.54	45.72	61.55	42.74	50.51	49.82		
o)				TF-IDF	(0, 0)	28.52	25.85	36.03	23.78	5.83	7.16
p)				word2vec	(0, 0)	29.03	27.44	37.31	25.08	13.83	13.43

Table 2: Results (omega index $\times 100$). Averaged over 10 runs.

demonstrates their effectiveness in adaptively focusing on different information, so as to cooperatively produce a meaningful utterance representation.

We also inspect in Fig. 7 the curve of normalized time-aware self-attention weights derived from the learned universal time-aware attention function. We also show the curves of the three components composing the universal function (see Eq. 13). We can see the mechanism automatically learned properly decaying curves for fitting the dialogue context, showing the most recent utterances are more important than the least recent ones with respect to the current utterance at time t . However the curves for the pre and post contexts are not symmetric and decay in different manners, revealing some interesting perspectives on the time distribution of salient information in dialogues. We can indeed observe that only a few succeeding utterances ($t + 1 \rightarrow t + 5$) seem to matter for understanding the current utterance, while for the pre-context, the importance decreases much more slowly as the distance increases. This suggests that even old utterances are still considerably helpful in understanding the current utterance.

7.4 Other discussions

Usage of discourse features. Discourse features are very helpful through our experiments. They are introduced into our model by concatenating at the word-level (see Section 4.2) instead of concatenating with the output of self-attention γ at the sentence-level. The decision is made based

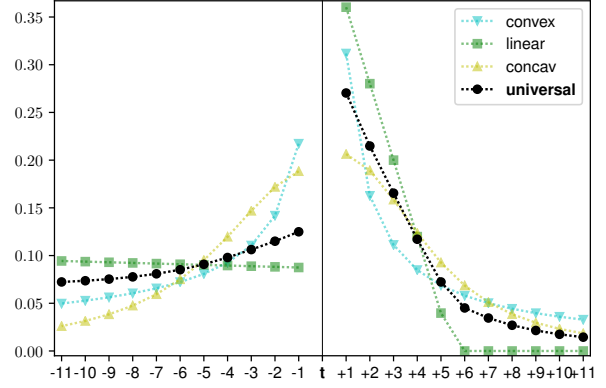


Figure 7: Normalized time-aware self-attention weights for pre and post contexts. Averaged over 10 runs.

on empirical results, moreover this is also aligned with the nature of word being part of transcription, which has richer meaning than just the word itself, thus its representation should be enriched with discourse features.

Simplified task. We also experimented on a much simpler task, where only the communities of type *abstract* were considered. This makes ACD much simpler, because the nested and overlapping cases are mainly associated with the other community types, as shown in Table 1. For this simplified task, we have 1147 unique communities, 78.99% of which are disjoint. *Our Model* achieves 72.09 in terms of $P@k = v$ and 55.67 in terms of Omega Index when $|Q| = v$. $P, R, F1@k = 15$ are respectively equal to 55.07, 74.37, and 54.00, and the Omega Index is 54.30 when $|Q| = 8$.

8 Conclusion

In this paper, we adopt an energy-based approach to the Abstractive Community Detection (ACD) task. We propose a novel contextual utterance encoder that capitalizes on three types of self-attention mechanisms, and test it within the powerful siamese and triplet meta-architectures against strong baselines. Experimental results demonstrate that our encoder improves on the state-of-the-art, and that energy-based modeling is well-suited to ACD. Moreover, we introduce a general triplet sampling scheme that we show enables the triplet architecture to learn subtle clustering patterns, such as overlapping and nested communities. This has many applications outside of ACD.

Acknowledgments

This research was supported in part by the OpenPaaS::NG and LinTo projects.

References

- Brandon Amos, Bartosz Ludwiczuk, and Mahadev Satyanarayanan. 2016. Openface: A general-purpose face recognition library with mobile applications. Technical report, CMU-CS-16-118, CMU School of Computer Science.
- Dzmitry Bahdanau, Kyunghyun Cho, and Yoshua Bengio. 2014. Neural machine translation by jointly learning to align and translate. *arXiv preprint arXiv:1409.0473*.
- Siddhartha Banerjee, Prasenjit Mitra, and Kazunari Sugiyama. 2015. [Generating abstractive summaries from meeting transcripts](#). In *Proceedings of the 2015 ACM Symposium on Document Engineering, DocEng '15*, pages 51–60, New York, NY, USA. ACM.
- James C. Bezdek, Robert Ehrlich, and William Full. 1984. [Fcm: The fuzzy c-means clustering algorithm](#). *Computers & Geosciences*, 10(2):191 – 203.
- Jane Bromley, Isabelle Guyon, Yann LeCun, Eduard Säckinger, and Roopak Shah. 1994. [Signature verification using a "siamese" time delay neural network](#). In J. D. Cowan, G. Tesauero, and J. Alspector, editors, *Advances in Neural Information Processing Systems 6*, pages 737–744. Morgan-Kaufmann.
- Kyunghyun Cho, Bart van Merriënboer, Caglar Gulcehre, Dzmitry Bahdanau, Fethi Bougares, Holger Schwenk, and Yoshua Bengio. 2014. [Learning phrase representations using rnn encoder–decoder for statistical machine translation](#). In *Proceedings of the 2014 Conference on Empirical Methods in Natural Language Processing (EMNLP)*, pages 1724–1734, Doha, Qatar. Association for Computational Linguistics.
- S. Chopra, R. Hadsell, and Y. LeCun. 2005. [Learning a similarity metric discriminatively, with application to face verification](#). In *2005 IEEE Computer Society Conference on Computer Vision and Pattern Recognition (CVPR'05)*, volume 1, pages 539–546 vol. 1.
- L. M. Collins and C. W. Dent. 1988. Omega: A general formulation of the rand index of cluster recovery suitable for non-disjoint solutions. *Multivariate Behavioral Research*, 23(2):231–242.
- Jacob Eisenstein and Regina Barzilay. 2008. [Bayesian unsupervised topic segmentation](#). In *Proceedings of the 2008 Conference on Empirical Methods in Natural Language Processing*, pages 334–343, Honolulu, Hawaii. Association for Computational Linguistics.
- Michel Galley, Kathleen R. McKeown, Eric Fosler-Lussier, and Hongyan Jing. 2003. [Discourse segmentation of multi-party conversation](#). In *Proceedings of the 41st Annual Meeting of the Association for Computational Linguistics*, pages 562–569, Sapporo, Japan. Association for Computational Linguistics.
- Nikhil Garg, Benoit Favre, Korbinian Reidhammer, and Dilek Hakkani-Tür. 2009. Clusterrank: a graph based method for meeting summarization. In *Tenth Annual Conference of the International Speech Communication Association*.
- Elad Hoffer and Nir Ailon. 2015. Deep metric learning using triplet network. In *International Workshop on Similarity-Based Pattern Recognition*, pages 84–92. Springer.
- Diederik P Kingma and Jimmy Ba. 2014. Adam: A method for stochastic optimization. *arXiv preprint arXiv:1412.6980*.
- Yann LeCun, Sumit Chopra, Raia Hadsell, Fu Jie Huang, and et al. 2006. A tutorial on energy-based learning. In *PREDICTING STRUCTURED DATA*. MIT Press.
- Yann LeCun and Fu Jie Huang. 2005. Loss functions for discriminative training of energy-based models. In *AISTATS 2005 - Proceedings of the 10th International Workshop on Artificial Intelligence and Statistics*, pages 206–213.
- Ji Young Lee and Franck Dernoncourt. 2016. [Sequential short-text classification with recurrent and convolutional neural networks](#). In *Proceedings of the 2016 Conference of the North American Chapter of the Association for Computational Linguistics: Human Language Technologies*, pages 515–520. Association for Computational Linguistics.

- Zhouhan Lin, Minwei Feng, Cicero Nogueira dos Santos, Mo Yu, Bing Xiang, Bowen Zhou, and Yoshua Bengio. 2017. A structured self-attentive sentence embedding. *arXiv preprint arXiv:1703.03130*.
- Jinchao Liu, Stuart J. Gibson, James Mills, and Margarita Osadchy. 2019. [Dynamic spectrum matching with one-shot learning](#). *Chemometrics and Intelligent Laboratory Systems*, 184:175 – 181.
- Thang Luong, Hieu Pham, and Christopher D. Manning. 2015. [Effective approaches to attention-based neural machine translation](#). In *Proceedings of the 2015 Conference on Empirical Methods in Natural Language Processing*, pages 1412–1421. Association for Computational Linguistics.
- J. MacQueen. 1967. [Some methods for classification and analysis of multivariate observations](#). In *Proceedings of the Fifth Berkeley Symposium on Mathematical Statistics and Probability, Volume 1: Statistics*, pages 281–297, Berkeley, Calif. University of California Press.
- Iain McCowan, Jean Carletta, W Kraaij, S Ashby, S Bourban, M Flynn, M Guillemot, T Hain, J Kadlec, V Karaiskos, et al. 2005. The ami meeting corpus. In *Proceedings of the 5th International Conference on Methods and Techniques in Behavioral Research*, volume 88.
- Yashar Mehdad, Giuseppe Carenini, Frank Tompa, and Raymond T. NG. 2013. [Abstractive meeting summarization with entailment and fusion](#). In *Proceedings of the 14th European Workshop on Natural Language Generation*, pages 136–146. Association for Computational Linguistics.
- Tomas Mikolov, Quoc V. Le, and Ilya Sutskever. 2013. [Exploiting similarities among languages for machine translation](#). *CoRR*, abs/1309.4168.
- Jonas Mueller and Aditya Thyagarajan. 2016. [Siamese recurrent architectures for learning sentence similarity](#). In *Proceedings of the Thirtieth AAAI Conference on Artificial Intelligence, AAAI’16*, pages 2786–2792. AAAI Press.
- Gabriel Murray, Giuseppe Carenini, and Raymond Ng. 2012. [Using the omega index for evaluating abstractive community detection](#). In *Proceedings of Workshop on Evaluation Metrics and System Comparison for Automatic Summarization*, pages 10–18. Association for Computational Linguistics.
- Gabriel Murray, Steve Renals, and Jean Carletta. 2005. Extractive summarization of meeting recordings. In *in Proceedings of the 9th European Conference on Speech Communication and Technology*, pages 593–596.
- Paul Neculoiu, Maarten Versteegh, and Mihai Rotaru. 2016. [Learning text similarity with siamese recurrent networks](#). In *Proceedings of the 1st Workshop on Representation Learning for NLP*, pages 148–157. Association for Computational Linguistics.
- Tatsuro Oya, Yashar Mehdad, Giuseppe Carenini, and Raymond Ng. 2014. [A template-based abstractive meeting summarization: Leveraging summary and source text relationships](#). In *Proceedings of the 8th International Natural Language Generation Conference (INLG)*, pages 45–53. Association for Computational Linguistics.
- F. Schroff, D. Kalenichenko, and J. Philbin. 2015. [Facenet: A unified embedding for face recognition and clustering](#). In *2015 IEEE Conference on Computer Vision and Pattern Recognition (CVPR)*, volume 00, pages 815–823.
- Veit Schwämmle and Ole Nørregaard Jensen. 2010. [A simple and fast method to determine the parameters for fuzzy c-means cluster analysis](#). *Bioinformatics*, 26(22):2841–2848.
- Abigail See, Peter J. Liu, and Christopher D. Manning. 2017. [Get to the point: Summarization with pointer-generator networks](#). In *Proceedings of the 55th Annual Meeting of the Association for Computational Linguistics (Volume 1: Long Papers)*, pages 1073–1083. Association for Computational Linguistics.
- Guokan Shang, Wensi Ding, Zekun Zhang, Antoine Tixier, Polykarpos Meladianos, Michalis Vazirgiannis, and Jean-Pierre Lorré. 2018. [Unsupervised abstractive meeting summarization with multi-sentence compression and budgeted submodular maximization](#). In *Proceedings of the 56th Annual Meeting of the Association for Computational Linguistics (Volume 1: Long Papers)*, pages 664–674. Association for Computational Linguistics.
- Karan Singla, Evgeny Stepanov, Ali Orkan Bayer, Giuseppe Carenini, and Giuseppe Riccardi. 2017. [Automatic community creation for abstractive spoken conversations summarization](#). In *Proceedings of the Workshop on New Frontiers in Summarization*, pages 43–47. Association for Computational Linguistics.
- Nitish Srivastava, Geoffrey Hinton, Alex Krizhevsky, Ilya Sutskever, and Ruslan Salakhutdinov. 2014. [Dropout: A simple way to prevent neural networks from overfitting](#). *Journal of Machine Learning Research*, 15:1929–1958.
- Shang-Yu Su, Pei-Chieh Yuan, and Yun-Nung Chen. 2018. [How time matters: Learning time-decay attention for contextual spoken language understanding in dialogues](#). In *Proceedings of the 2018 Conference of the North American Chapter of the Association for Computational Linguistics: Human Language Technologies, Volume 1 (Long Papers)*, pages 2133–2142. Association for Computational Linguistics.
- Antoine Tixier, Polykarpos Meladianos, and Michalis Vazirgiannis. 2017. [Combining graph degeneracy and submodularity for unsupervised extractive summarization](#). In *Proceedings of the Workshop on New Frontiers in Summarization*, pages 48–58. Association for Computational Linguistics.

Ashish Vaswani, Noam Shazeer, Niki Parmar, Jakob Uszkoreit, Llion Jones, Aidan N Gomez, Łukasz Kaiser, and Illia Polosukhin. 2017. Attention is all you need. In *Advances in Neural Information Processing Systems*, pages 5998–6008.

Jiang Wang, Yang Song, Thomas Leung, Chuck Rosenberg, Jingbin Wang, James Philbin, Bo Chen, and Ying Wu. 2014. [Learning fine-grained image similarity with deep ranking](#). In *Proceedings of the 2014 IEEE Conference on Computer Vision and Pattern Recognition, CVPR '14*, pages 1386–1393, Washington, DC, USA. IEEE Computer Society.

Zichao Yang, Diyi Yang, Chris Dyer, Xiaodong He, Alex Smola, and Eduard Hovy. 2016. [Hierarchical attention networks for document classification](#). In *Proceedings of the 2016 Conference of the North American Chapter of the Association for Computational Linguistics: Human Language Technologies*, pages 1480–1489. Association for Computational Linguistics.

Supplementary Material

Appendices

A Triplet sampling scheme

Recall that for a given triplet (pos, anc, neg) (positive, anchor, negative), the objective of training is to make the distance between pos and anc much smaller than the distance between anc and neg . We construct triplets by considering community pairs. For a meeting that includes N unique communities, we have $\binom{N}{2}$ unique pairs of them. A given pair of communities can either (1) be disjoint, i.e., not have any element in common (Fig. 8a), (2) be nested in one another (top of Fig. 8b), or (3) overlap. Our triplet sampling scheme needs to account for these three cases so that the learned embedding space encodes a meaningful distance that can recover such fine patterns.

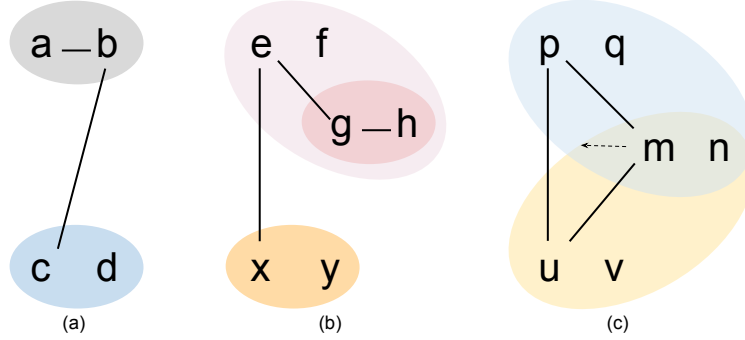


Figure 8: (a) communities $\{a, b\}$ and $\{c, d\}$ are disjoint (b) community $\{g, h\}$ is nested in community $\{e, f, g, h\}$ (c) communities $\{p, q, m, n\}$ and $\{m, n, u, v\}$ overlap upon $\{m, n\}$.

A.1 Disjoint case

As shown in Fig. 8a, let us consider two communities $\{a, b\}$ and $\{c, d\}$ that do not share any element. We can derive 8 triplets from these two communities:

$(a, b, c), (b, a, c), (a, b, d), (b, a, d), (c, d, a), (d, c, a), (c, d, b), (d, c, b)$.

As a result of passing these triplets to the network, the intra-community distances are reduced while the inter-community distances are enlarged. Note that (a, b, c) and (b, a, c) are considered different triplets, as they involve different sides of the same triangle.

To formalize, we denote the set of all 2-permutations of a set S by $Permu(S, 2) = \{(i, j) : i, j \in S, i \neq j\}$, and the number of such permutations as $P_2^{|S|} = \frac{(|S|)!}{(|S|-2)!}$, where $|*|$ denotes cardinality. Note that when $|S| = 1$, (singleton community), we repeat the single element of $S = \{i\}$, thus $Permu(S, 2) = \{(i, i)\}$. The Cartesian product of two sets $S1$ and $S2$ is denoted as $Carte(S1, S2) = \{(i, j) : i \in S1, j \in S2\}$, the universal set of all elements as Ω (union of all communities), and the empty set as \emptyset .

For any two disjoint communities, i.e., $A \cap B = \emptyset$, the complete set of sampled triplets is:

$$\begin{aligned} & \{(pos, anc, neg) : (pos, anc) \in Permu(A, 2), neg \in B\} \\ & \cup \{(pos, anc, neg) : (pos, anc) \in Permu(B, 2), neg \in A\} \end{aligned} \quad (15)$$

The corresponding number of triplets is $P_2^{|A|} \times |B| + P_2^{|B|} \times |A|$.

A.2 Nested case

As shown in Fig. 8b, community $\{g, h\}$ is nested in community $\{e, f, g, h\}$. We first create triplets by comparing the nested part $\{g, h\}$ with $\{e, f, g, h\} \setminus \{g, h\} = \{e, f\}$ like in the previous case, which ensures e.g., that $d_{hg} \ll d_{ge}, d_{ef} \ll d_{fh}$, etc. Additionally, an extra constraint should be added to the

edges linking the two above parts, (such as d_{ge}), in order to guarantee, e.g., that g is closer to e than to any utterance from any other disjoint community (e.g., x or y). That is, we want $d_{ge} \ll d_{ex}$. Therefore, we create the following extra triplets:

$$(e, g, x), (g, e, x), (e, g, y), (g, e, y), (e, h, x), (h, e, x), (e, h, y), (h, e, y) \\ (f, g, x), (g, f, x), (f, g, y), (g, f, y), (f, h, x), (h, f, x), (f, h, y), (h, f, y).$$

To formalize, for any two nested communities, e.g. $A \subset B$, the complete set of sampled triplets is:

$$\begin{aligned} & \{(pos, anc, neg) : (pos, anc) \in Carte(A, B \setminus A), neg \in \Omega \setminus B\} \\ & \cup \{(pos, anc, neg) : (pos, anc) \in Carte(B \setminus A, A), neg \in \Omega \setminus B\} \\ & \cup \{(pos, anc, neg) : (pos, anc) \in Permu(A, 2), neg \in B \setminus A\} \\ & \cup \{(pos, anc, neg) : (pos, anc) \in Permu(B \setminus A, 2), neg \in A\} \end{aligned} \quad (16)$$

The corresponding number of triplets is $P_2^{|A|} \times |B \setminus A| + P_2^{|B \setminus A|} \times |A| + |A| \times |B \setminus A| \times |\Omega \setminus B| \times 2$.

A.3 Overlapping case

As shown in Fig. 8c, two communities may also overlap. E.g., $\{p, q, m, n\}$ and $\{m, n, u, v\}$ overlap upon $\{m, n\}$. We first consider this overlapping case as two nested cases: $\{m, n\}$ nested in $\{p, q, m, n\}$ and $\{m, n\}$ nested in $\{m, n, u, v\}$. We thus sample triplets as explained in A.2. However, here, we also have the extra constraint that the overlap $\{m, n\}$ be pulled in-between $\{p, q\}$ and $\{u, v\}$, as shown by the dashed arrow in Fig. 8c. To capture this, we include these additional triplets:

$$(m, p, u), (m, u, p), (m, p, v), (m, v, p), (m, q, u), (m, u, q), (m, q, v), (m, v, q) \\ (n, p, u), (n, u, p), (n, p, v), (n, v, p), (n, q, u), (n, u, q), (n, q, v), (n, v, q).$$

To formalize, for any two overlapping communities A and B , i.e., $A \cap B \neq \emptyset, A \neq B, A \not\subset B, B \not\subset A$, these additional triplets correspond to:

$$\begin{aligned} & \{(pos, anc, neg) : (pos, anc) \in Carte(A \cap B, A \setminus B), neg \in B \setminus A\} \\ & \cup \{(pos, anc, neg) : (pos, anc) \in Carte(A \cap B, B \setminus A), neg \in A \setminus B\} \end{aligned}$$

$$\begin{aligned} & \cup \{(pos, anc, neg) : (pos, anc) \in Permu(A \setminus B, 2), neg \in B \setminus A\} \\ & \cup \{(pos, anc, neg) : (pos, anc) \in Permu(B \setminus A, 2), neg \in A \setminus B\} \end{aligned}$$

And, as was previously mentioned, we also consider two nested cases:

$$\begin{aligned} & \cup \{(pos, anc, neg) : (pos, anc) \in Permu(A \setminus B, 2), neg \in A \cap B\} \\ & \cup \{(pos, anc, neg) : (pos, anc) \in Permu(A \cap B, 2), neg \in A \setminus B\} \\ & \cup \{(pos, anc, neg) : (pos, anc) \in Carte(A \setminus B, A \cap B), neg \in \Omega \setminus (A \cup B)\} \\ & \cup \{(pos, anc, neg) : (pos, anc) \in Carte(A \cap B, A \setminus B), neg \in \Omega \setminus (A \cup B)\} \end{aligned} \quad (17)$$

$$\begin{aligned} & \cup \{(pos, anc, neg) : (pos, anc) \in Permu(B \setminus A, 2), neg \in A \cap B\} \\ & \cup \{(pos, anc, neg) : (pos, anc) \in Permu(A \cap B, 2), neg \in B \setminus A\} \\ & \cup \{(pos, anc, neg) : (pos, anc) \in Carte(B \setminus A, A \cap B), neg \in \Omega \setminus (A \cup B)\} \\ & \cup \{(pos, anc, neg) : (pos, anc) \in Carte(A \cap B, B \setminus A), neg \in \Omega \setminus (A \cup B)\} \end{aligned}$$

The corresponding total number of triplets is :

$$\begin{aligned} & (P_2^{|A \setminus B|} \times |A \cap B| + P_2^{|A \cap B|} \times |A \setminus B| + |A \setminus B| \times |A \cap B| \times |\Omega \setminus (A \cup B)| \times 2) \\ & + (P_2^{|B \setminus A|} \times |A \cap B| + P_2^{|A \cap B|} \times |B \setminus A| + |B \setminus A| \times |A \cap B| \times |\Omega \setminus (A \cup B)| \times 2) \\ & + (P_2^{|A \setminus B|} \times |B \setminus A| + P_2^{|B \setminus A|} \times |A \setminus B|) \\ & + (|A \cap B| \times |A \setminus B| \times |B \setminus A| \times 2) \end{aligned} \quad (18)$$

A.4 Visualization

Our triplet sampling scheme is effective if it can make the triplet architecture learn an embedding space in which distances capture basic community structure (disjoint case) and the two more subtle nested and overlapping cases. In order to test its effectiveness, we inspect what happens for the IS1001c meeting, which includes 12 abstractive communities and 48 unique utterances. 23612 triplets can be sampled with our approach.

We trained our model on this set of triplets for 5 epochs. The utterance embeddings projected onto the first two PCA dimensions are shown in Fig. 9, in which the utterances belonging to the same ground truth community are encircled by an ellipse. We can observe that utterances are placed at the right places as desired, such as:

- overall, utterances belonging to the same community are close to each other (small intra-community distances), and disjoint communities are far from each other (large inter-community distances).
- In the upper right corner of Fig. 9, the nested part and the community in which that part is nested are well separated, but they are closer to each other than to any other disjoint community.
- In the center of Fig. 9, the overlap has successfully been pulled in-between the two overlapping communities.

This provides evidence that, with well-designed triplets, it is possible to learn a space encoding very fine clustering patterns with the triplet network. To the best of our knowledge, this is novel and has never been proven by prior literature. Moreover, our proposed triplet sampling scheme is general and can thus be applied to any task where a rich metric needs to be learned to encode subtle grouping information.

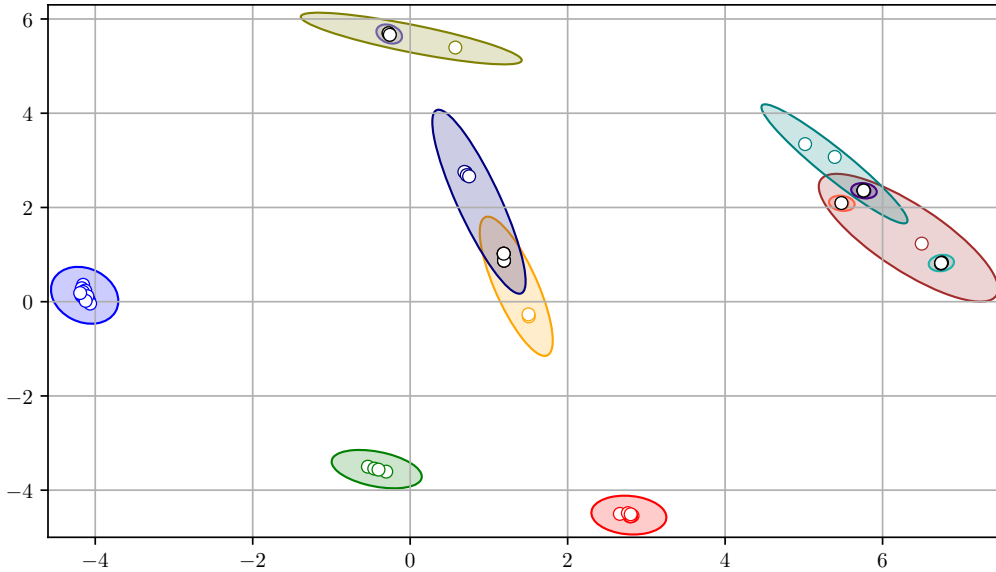


Figure 9: All 48 utterances of 12 abstractive communities from the meeting IS1001c projected into 2-dimensional PCA of learned 32-dimensional embedding space. Trained on 23612 triplets for 5 epochs. Converged $P@k = v$ is equal to 96.33%

The embedding space can also be interactively explored. We provide the following link to Embedding Projector, corresponding to a more complicated example with more elements and communities (the ES2016b meeting) learned in the same way as in the previous example.

<https://projector.tensorflow.org/?config=https://gist.githubusercontent.com/shangguokan/fb859f90563369cc6b01e7897ec6fb37/raw/063f2429f46cee13896a66a9aae059934aef16a2/ES2016b.json>

B Attention visualization

The aim of this section is to show, with an example, what the three self-attention mechanisms pay attention to while encoding the current utterance U^t . Fig. 10 shows the attention distributions over U^t (highlighted by the black frame), and over its pre context $\{U^{t-1}, \dots, U^{t-11}\}$ and post context $\{U^{t+1}, \dots, U^{t+11}\}$ utterances. We use three colors that are consistent with the ones used in Fig. 5 to denote the three different attention mechanisms: green for content-aware (α), blue for time-aware (β), and red for basic self-attention (γ). Remember that α and β are both in the context encoder, while γ is in the utterance encoder. Color shades indicate attention intensity (the darker, the stronger).

-11	ID:	And	we'll	need	to	custom	desi	design	a	circuit	board	,			
-10	ID:	because	the	circuit	board	has	to	take	the	button	input	and	send	it	to ...
-9	ID:	But	once	we	come	up	with	a	design	we'll	send	it	to	the	circuit ...
-8	ID:	Um	,	standard	parts	include	the	buttons	and	the	wheels	,	um	the	iPod-style ...
-7	ID:	The	infrared	LED	is	actually	gonna	be	included	in	the	circuit	board	that	comes ...
-6	ID:	Um	,	we	need	a	radio	sender	and	receiver	,	those	are	standard	.
-5	ID:	And	al	we	also	need	a	beeper	or	buzzer	or	other	sort	of	noise ...
-4	ID:	So	we	have	some	material	options	.							
-3	ID:	Um	,	we	can	use	rubber	,	plastic	,	wood	or	titanium	.	
-2	ID:	Um	,	I'd	recommend	against	titanium								
-1	ID:	because	it	can	only	be	used	in	the	flat	cases	and	it's	really	heavy .
t	ID:	PRE	Um	,	and	the	rubber	case	requires	rubber	buttons	,	so	if	we definitely
		want	plastic	buttons	,	we	shouldn't	have	a	rubber	case	.	POST		
+1	PM:	And	why	not	wood	?									
+2	ID:	And													
+3	ID:	hmm	?												
+4	PM:	And	why	not	wood	?									
+5	ID:	Uh	,	well	we	can	use	wood	.						
+6	ID:	I	don't	know	why	we'd	want	to	.						
+7	ID:	Um	and	also	we	should	note	that	if	we	want	an	iPod-style	wheel	button ...
+8	ID:	We	can't	use	the	minimal	chip	,	we	need	the	next	higher	grade	, ...
+9	ID:	I	don't	think	it's	much	more	expensive	,	but	it	is	more	expensive	.
+10	ID:	So	that's	what	I've	got	on	design	.						
+11	PM:	'S	good	.											

Figure 10: Visualization of attention distributions around an utterance from the ES2011c meeting. Some utterances are truncated for readability.

We can observe in Fig. 10 that:

- the content-aware self-attention mechanism α focuses on the informative and complementary words in the contexts that are central to understanding the utterance at time t , such as: “custom”, “design” from U^{t-11} , “material” from U^{t-4} , “recommend”, “titanium” from U^{t-2} , “wood” from U^{t+1} , etc.
- the time-aware self-attention mechanism β places more importance over the context utterances that close to U^t , i.e., the importance decreases when the time distance increases. However, this follows different patterns for the pre and post contexts, as was discussed in Subsection 7.3).
- the self-attention mechanism γ concentrates mainly on the special pre-context token PRE, meaning that the pre-context is more important than the post-context in the example considered. Generally speaking, the pre and post context tokens contain richer information than any token from the current utterance, as the context tokens originate from the fusion of $\{U^{t-11}, \dots, U^t, \dots, U^{t+11}\}$. It is thus possible that the utterance encoder has learned to always pay more attention to these information-rich tokens than to any regular token.

- it is also interesting to note that considerable attention is being paid to punctuation marks. This makes sense, since they are important pieces of information indicative of utterance type (e.g. statement or question).

To summarize, the visualization results show that the three self-attention mechanisms of our model are able to adaptively focus on different information, in order to cooperatively produce a meaningful representation.

C Details about the FCM algorithm

More precisely, the goal is to minimize the weighted within group sum of squared error objective function:

$$J(M, Q) = \sum_{q=1}^{|Q|} \sum_{t=1}^T (m_{qt})^{fuz} \|\mathbf{u}^t - \mathbf{c}_q\|_2^2 \quad (19)$$

where M and Q are the sets of membership probability distributions and community centroid vectors, $m_{qt} \in [0, 1]$ is the probability that the t -th utterance belongs to the q -th community (with $\sum_{q=1}^{|Q|} m_{qt} = 1$), fuz is a parameter that controls the amount of fuzziness, $\|\cdot\|_2$ denotes the Euclidean distance in the triplet case (we replace it with Manhattan distance $\|\cdot\|_1$ in the siamese case), \mathbf{u}^t is the t -th utterance vector, and \mathbf{c}_q is the q -th community centroid vector.

M and Q are iteratively updated with equations:

$$m_{qt} = \left(\sum_{j=1}^{|Q|} \left(\frac{\|\mathbf{u}^t - \mathbf{c}_q\|_2}{\|\mathbf{u}^t - \mathbf{c}_j\|_2} \right)^{\frac{2}{fuz-1}} \right)^{-1} \quad (20)$$

$$\mathbf{c}_q = \frac{\sum_{t=1}^T (m_{qt})^{fuz} \mathbf{u}^t}{\sum_{t=1}^T (m_{qt})^{fuz}} \quad (21)$$

When $fuz \rightarrow +\infty$, $\forall q \in |Q|$, $\forall t \in T$, m_{qt} tends to be equal to $1/|Q|$, thus utterances have identical membership to each community. While when $fuz \rightarrow 1$, FCM becomes equivalent to traditional k -means, in which m_{qt} is either 0 or 1 for a given utterance \mathbf{u}^t and community centroid \mathbf{c}_q . Usually in practice, $fuz = 2$ (Schwämmle and Jensen, 2010). Learning stops until the maximum number of iterations is reached or $J(M, Q)$ decreases by less than a predefined threshold. Moreover, due to its stochastic nature, we run the algorithm 20 times with different random initializations and select the run yielding the smallest objective function value.

D Ranking example

With respect to the given utterance from the ES2011c meeting in below, we show the list of other utterances ordered from the closest to the farthest, in terms of Euclidean distance. The other utterances that belong to the same community of the give utterance are highlighted in bold. For this example, $P@k = v$ is equal to 77.78, where $v = 9$. $P, R, F1@k = 10$ are 80.00, 88.89, 84.21 respectively.

ID: Um , and the rubber case requires rubber buttons , so if we definitely want plastic buttons , we shouldn't have a rubber case .

- 0.11 ID: Um , we can use rubber , plastic , wood or titanium .
- 0.12 **ID: And al we also need a beeper or buzzer or other sort of noise thing for locating the remote .**
- 0.38 **ID: Um , I'd recommend against titanium**
- 0.42 ID: Um and also we should note that if we want an iPod-style wheel button , it's gonna require a m qu slightly more expensive chip .
- 0.54 **ID: Uh , well we can use wood .**
- 0.57 **ID: Um , standard parts include the buttons and the wheels , um the iPod-style wheel .**
- 0.68 **ID: I don't know why we'd want to .**
- 0.96 **ID: And we'll need to custom desi design a circuit board ,**
- 1.26 **ID: Um , I assume we'll be custom designing our case ,**
- 1.27 **ID: Um , so we need some custom design parts , and other parts we'll just use standard .**
- 1.43 **ID: So I've been looking at the components design .**

1.66	ME: Um , can I do next ? Because I have to say something about the material
2.24	ME: and the findings are that the first thing to aim for is a fashion uh , fancy look and feel .
2.57	ME: Um . Next comes technologic technology and the innovations to do with that .
3.21	ME: And th last thing is the easy to use um factor .
3.92	UI: Uh , so people are going to be looking at this little screen .
4.02	ME: But the screen can come up on the telly , the she said .
...	
8.81	ID: It didn't give me any actual cost .
8.84	ID: All it said was it gave sort of relative , some chips are more expensive than others , sort of things .
8.89	ME: So if you throw it , it's gonna store loads of energy , and you don't need to buy a battery because they're quite f I find them annoying .
9.00	ME: But we need to find cost .
9.06	ME: Does anyone have costs on the on the web ?
9.95	PM: And you're gonna be doing protu product evaluation .
9.96	PM: Oh when we move on , you two are going to be playing with play-dough .
10.15	PM: Um , and working on the look and feel of the design and user interface design .

This abstractive community of 10 utterances is summarized into the abstractive sentence: The Industrial Designer gave her presentation on components and discussed which would have to be custom-made and which were standard.

E Omega Index

The Omega Index evaluates the *degree of agreement* between two clustering solutions based on *pairs* of objects being clustered. Two solutions s_1 and s_2 are considered to agree on a given pair of objects, if two objects are placed by both solutions in *exactly* the same *number of communities* (possibly zero).

The Omega Index ω is computed as shown in Equation 22. The numerator is the observed agreement ω_{obs} adjusted by expected (chance) agreement ω_{exp} , while the denominator is the perfect agreement (value equals to 1) adjusted by expected agreement.

$$\omega(s_1, s_2) = \frac{\omega_{obs}(s_1, s_2) - \omega_{exp}(s_1, s_2)}{1 - \omega_{exp}(s_1, s_2)} \quad (22)$$

Observed and expected agreements are calculated as below:

$$\omega_{obs}(s_1, s_2) = \frac{1}{N} \sum_{j=0}^{\min(J,K)} A_j \quad (23)$$

$$\omega_{exp}(s_1, s_2) = \frac{1}{N^2} \sum_{j=0}^{\min(J,K)} N_{j1} N_{j2} \quad (24)$$

where A_j is the number of pairs agreed to be assigned to j number of communities by both solutions, N_{j1} is the number of pairs assigned to j communities in s_1 , N_{j2} is the number of pairs assigned to j communities in s_2 , J and K represent respectively the maximum number of communities in which any pair of objects appear together in solutions s_1 and s_2 , and $N = n(n-1)/2$ is the total number of pairs constructed over n number of objects.

To give an example, consider two clustering solutions for 5 objects:

$$\begin{aligned} s_1 &= \{\{a, b, c\}, \{b, c, d\}, \{c, d, e\}, \{c, d\}\} \\ s_2 &= \{\{a, b, c, d\}, \{b, c, d, e\}\} \end{aligned}$$

	solution s_1	solution s_2	solutions
	#communities	#communities	s_1 and s_2
	the pair is assigned	the pair is assigned	agree on the pair?
(a, b)	1	1	yes
(a, c)	1	1	yes
(a, d)	0	1	no
(a, e)	0	0	yes
(b, c)	2	2	yes
(b, d)	1	2	no
(b, e)	0	1	no
(c, d)	3	2	no
(c, e)	1	1	yes
(d, e)	1	1	yes

Solutions are transformed into the table above, from what we can obtain $N = 10, J = 3, K = 2, \min(J, K) = 2$. Two solutions agree to place (a, e) together in no community, the pairs (a, b) , (a, c) , (c, e) and (d, e) in one community, and the pair (b, c) in two communities. We have $A_0 = 1, A_1 = 4, A_2 = 1$. Thus the observed agreement is $(1 + 4 + 1)/10 = 0.6$. Since $N_{01} = 3, N_{11} = 5, N_{21} = 1$ and $N_{02} = 1, N_{12} = 6, N_{22} = 3$, the expected agreement then is $(3 * 1 + 5 * 6 + 1 * 3)/10^2 = 0.36$. Finally, Omega Index for this simple example is computed as: $\omega(s_1, s_2) = (0.6 - 0.36)/(1 - 0.36) = 0.375$.